Mat. Res. Soc. Symp. Proc. Vol. 740 © 2003 Materials Research Society

Plasticity in Nanomaterials

Guo-Dong Zhan, Joshua D. Kuntz, Julin Wan, and Amiya K. Mukherjee
Department of Chemical Engineering and Materials Science
University of California, One Shields Avenue, Davis, CA 95616

ABSTRACT

There have been many predictions of the reinforcing effects of carbon nanotubes in various composite matrices but large improvements in properties have not yet been convincingly demonstrated. In the present study, we have successfully realized this possibility in reinforcing nanocrystalline alumina. Fully dense single-wall carbon nanotubes (SWCN)/Al_2O_3 nanocomposites with nanocrystalline alumina matrix have been fabricated at sintering temperatures as low as 1150°C by spark-plasma-sintering (SPS). A fracture toughness of 9.7 $MPam^{1/2}$, nearly three times that of pure nanocrystalline alumina, has been achieved in the 10 vol.% SWCN/Al_2O_3 nanocomposite. Moreover, high-strain-rate superplasticity has been achieved in $Al_2O_3/ZrO_2/MgAl_2O_4$ nanocomposite with truly nanocrystalline grain size of 100 nm. Compression superplastic tests were conducted in the temperature range of 1300-1450°C at strain rates 10^{-3}-10^{-1} s^{-1}. The results generated a stress exponent of ~ 2 and an activation energy of ~ 620 kJ/mol.

INTRODUCTION

The fabrication of nanocrystalline materials is an exciting area of materials research because such bulk materials with grain sizes less than 100 nm exhibit novel properties as compared with their microcrystalline counterparts, such as optical transparency and enhanced superplasticity. However, the brittleness of nanocrystalline ceramics has limited their potential and promise for use in structural applications. Carbon nanotubes, especially single-wall carbon nanotubes (SWCN), should be ideal reinforcing fibers for composites [1]. Theoretical and experimental studies [2,3] showed that carbon nanotubes with very high aspect ratios (length-to-diameter ratio of 1,000 or more) have exceptional mechanical characteristics. SWCN are among the stiffest fibers known, with a measured Young's modulus of ~1.5 TPa [4]. However, to date, the utilization of the extraordinary mechanical properties of carbon nanotubes in composites has not been successfully realized, e.g., in alumina based systems only a 24% increase in toughness has been obtained so far. In the present study, we have successfully realized the potential of carbon nanotubes in significantly reinforcing ceramics for the first time.

Superplasticity is another exciting area for nanocrystalline ceramic materials. High strain rate superplasticity (HSRS) is usually referred to as the demonstration of high ductility at strain rates around 10^{-2} s^{-1} or greater [5,6] . HSRS used to be a phenomenon found exclusively in fine-grained metals and metal matrix composites. For ceramics, the typical superplastic strain rate is in the range of 10^{-5}-10^{-4} s^{-1}. Ceramic HSRS was not observed until very recently [7,8]. Kim et al. [7] reported a composite ceramic material consisting of tetragonal ZrO_2, $MgAl_2O_4$ and α-Al_2O_3 phases that exhibit superplasticity at strain rates up to 1 s^{-1} at 1650°C. While scientifically significant, these results are not of practical importance due to the prohibitively high forming temperature. Additionally, these results did not provide any phenomenological data to account for a deformation mechanism. In the present work, we strive to bring the HSRS deformation

temperature for this triphasic ceramic to 1350°C or lower. Tests were also conducted to establish the strain-rate sensitivity and activation energy of the deformation process, which are two of the three primary characteristic rate parameters required for further modeling of the deformation phenomenon.

EXPERIMENTAL

The alumina powder used in the alumina-SWCN composites, consisting of 80% α-Al_2O_3 and 20% γ-Al_2O_3 with particle sizes of 300 nm (40 nm crystallite size) and 20 nm respectively, was obtained from Baikowski International Corporation (Charlotte, NC 28273). Purified single-wall carbon nanotubes (also called Buckytubes) were obtained from Carbon Nanotechnologies Incorporated (Houston, TX 77084). The SWCN were produced by the HiPco process [9,10] . Two compositions, containing SWCN at 5.7 vol.% and 10 vol.%, were produced. For the superplasticity investigation, the material is targeted the same overall phase composition as reported by Kim et al.: 30 vol.%Al_2O_3, 40 vol.%ZrO_2 and 30 vol.%$MgAl_2O_4$. The starting materials were commercially available nano-sized powders: γ-Al_2O_3 (Nanotechnologies, Austin, TX), with 15 nm particle size; tetragonal ZrO_2 stabilized by 3 mol.% Y_2O_3 (Tosoh, Tokyo, Japan), with 24 nm particle size; MgO (Nanopowder Enterprise Inc., Piscataway, NJ), with 40 nm particle size. The powders were mixed by ball milling for 24 hours using zirconia media in ethanol. The mixed powder is pressed into a 19mm diameter graphite die and sintered with Dr. Sinter® 1050 spark plasma sintering system (Sumitomo Coal Mining Company, Ltd.) under vacuum. After applying the given pressure (63MPa), samples were heated to desired temperatures and held for a few minutes before turning off the power.

The final densities of the sintered compacts were determined by the Archimedes' method. Microstructural observation was carried out using high-resolution scanning electron microscope (SEM). Grain sizes were estimated from XRD and SEM analysis. Additional characterization by analytical electron microscopy and high-resolution transmission electron microscopy (HRTEM) was performed on a Philips CM-200. Indentation tests were performed on a Wilson Tukon hardness tester with a diamond Vickers indenter. The indentation parameters for fracture toughness (K_{IC}) and hardness measurements were a 2.5 Kg load with a dwell of 15 seconds. The fracture toughness was calculated by Antis equation [11].

In the superplasticity investigation, samples with dimensions 5 mm ×3 mm ×3 mm were machined from the sintered material, and subjected to compression tests on a computer-interfaced hydraulic testing machine. Computer control was used to run constant strain-rate tests and step strain-rate tests. The tests were performed in air; in the temperature range of 1300 - 1450°C and strain-rate range 10^{-3}-10^{-1} s^{-1}. Constant strain rate testing was realized by adjusting (decreasing) the crosshead speed in accordance with the instantaneous height of the specimen. These tests were terminated once a pre-set strain was reached. Step-strain rate tests were also conducted in constant strain-rate mode for each segment of the deformation, while the strain-rate was increased to the next higher rate when the strain reached 0.1 at each designated strain rate.

RESULTS AND DISCUSSION

Single-Walled Carbon Nanotubes Toughening

The processing conditions, physical and mechanical properties for pure alumina and nanocomposites are shown in Table I. The pure alumina nanopowders can be consolidated by SPS at 1150°C for 3 minutes to get full density. The microstructure of the pure Al_2O_3 consisted of equiaxed grains with an average value of 349 nm. Measured Vickers hardness and fracture toughness are 20.3 GPa and 3.3 $MPam^{1/2}$, respectively. Note that both 5.7 vol.% SWCN/Al_2O_3 and 10 vol.% SWCN/Al_2O_3 nanocomposites can also be successfully consolidated to their theoretical densities at the same sintering conditions as that for pure alumina, suggesting that the addition of SWCN to the alumina matrix was not detrimental to the sintering process. XRD analysis of the consolidated specimens reveals that the γ-Al_2O_3 has been transformed to α-Al_2O_3 in both the pure alumina and the composites. Most of the alumina grains were in the nanocrystalline range, around 200 nm. It is interesting to note that the introduction of carbon nanotubes leads to refinement of grain size. This refinement is consistent with observations by Laurent et al. [12]. The fracture toughness of the 5.7 vol.% SWCN/Al_2O_3 nanocomposite is over two times higher than that of pure alumina and there is almost no decrease in hardness. A toughness of nearly three times pure alumina was achieved in the 10 vol.% SWCN/Al_2O_3 nanocomposite when sintered under the same conditions. In the open literature [13,14], all the other carbon nanotubes reinforced ceramic composites have been consolidated by hot-pressing methods that require higher temperatures and longer duration than SPS. These sintering parameters must damage the carbon nanotubes in the composites, leading to decreases or total loss in reinforcing effects.

Table I. Processing conditions and the resultant properties of SWCN reinforced nanocrystalline alumina nanocomposites consolidated by spark-plasma-sintering

Materials	Processing conditions	Relative density (%TD)	Grain size (nm)	H_V (GPa)	K_{IC} ($MPam^{1/2}$)
Al_2O_3	SPS 1150°C/3 min.	100	349	20.3	3.3
5.7 vol.% SWCN/Al_2O_3	SPS 1150°C/3 min.	100	~200	20.0	7.9
10 vol.% SWCN/Al_2O_3	SPS 1150°C/3 min.	100	~200	16.1	9.7

Figure 1 shows the dependence of toughness on carbon nanotube content in the alumina nanocomposites. No reinforcing effect was noted in the *in-situ* carbon nanotubes-Fe-Al_2O_3 nanocomposites although the fracture toughness is similar to that of alumina. Moreover, only a marginal increase in fracture toughness can be obtained even by improving the quality and quantity of carbon nanotubes in the latter work [15] . The reasons given were mainly related to the damage of carbon nanotubes during hot-pressing. Also noted was the fact that volume contents of carbon nanotubes in the sintered products are lower than those in the starting powders. So far, the best reported result by Siegel et al. [13] was a 24% increase in toughness in 10 vol.% MWCN/Al_2O_3 nanocomposite. However, it can be seen that fracture toughness increases significantly with the introduction of single-wall carbon nanotubes for the present nanocomposites. The 10 vol.% SWCN/Al_2O_3 nanocomposite is nearly three times as tough as pure nanocrystalline alumina. To date, it is the best result achieved.

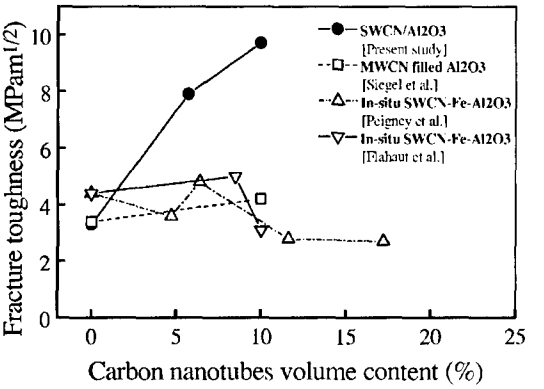

Figure 1. Fracture toughness versus carbon nanotube volume content in alumina based composites as reported in literature

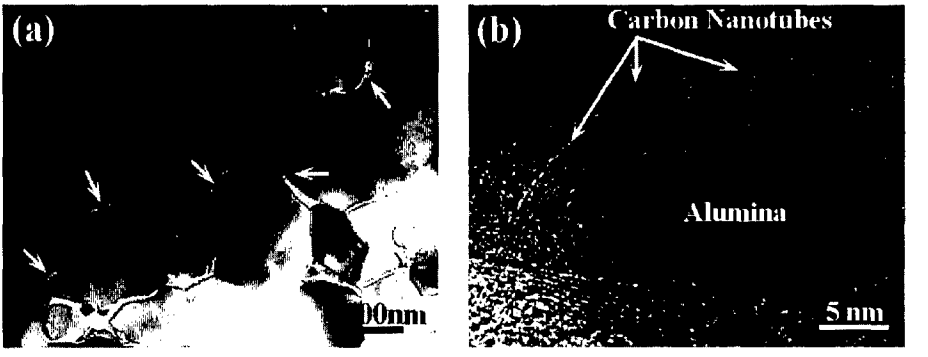

Figure 2. TEM Micrographs of 5.7 vol.% SWCN/Al_2O_3 nanocomposite. (a) Bright-field TEM image and (b) high-resolution TEM image of specimens in the fully dense 5.7 vol.% SWCN/Al_2O_3 nanocomposite. The arrows indicate the SWCN phase.

Figure 2a shows a typical bright field TEM image of the 5.7 vol.% SWCN/Al_2O_3 nanocomposite. It is interesting to note that carbon nanotubes were distributed along grain boundaries to develop a network microstructure. It can be seen that some of carbon nanotubes were entangled with alumina grains and some of them encapsulated alumina nano-scale grains. Intimate contact between carbon nanotubes and alumina was observed in this material, as shown in Figure 2b. XDS profile and spot scans were performed to analyze the chemical composition of the different grains, grain boundaries, and particles in the samples. The interface condition and bonding between the SWCN ropes and the alumina matrix are part of our ongoing study. The present results suggest that the extent of interfacial bonding might be a factor in increasing the toughness of the composites.

High Strain Rate Superplasticity

The microstructure of the as-sintered material is shown in Fig. 3. The material reached 4.63 g/cm^3 (100% theoretical density) after sintering for 3 minutes at 1150°C. XRD results identified the phases as t-ZrO_2, α-Al_2O_3 and $MgAl_2O_4$. The mean grain size is about 100 nm, about half the size of the material reported by Kim et al. [7]. The deformed sample shows larger grain size as compared to the original microstructure. The grain growth, however, has been determined to be mainly due to the time at temperature and not due to the deformation process. Stress-strain results indicate that at lower strain rates, the material undergoes moderate strain hardening (increasing of stress with strain); at intermediate rates, the flow stress remains relatively constant during deformation. At high strain-rates, there is an apparent strain softening (decreasing stress with increasing strain). The strain-hardening effect can be attributed to concurrent grain growth during superplastic deformation and was observed in the high temperature/low strain rate combinations. Strain softening, as established for metallic materials, is most likely to be caused by dynamic re-crystallization, and occurs in the low temperature/high strain rate combinations. In tensile tests, it has also been associated with cavitation. Constant stress deformation at a function of strain can be reached when these two effects balance each other, thus it is observed at intermediate strain rates.

Figure 3. SEM image of fractured surface of SPS-derived $Al_2O_3/ZrO_2/MgAl_2O_4$ nanocomposite

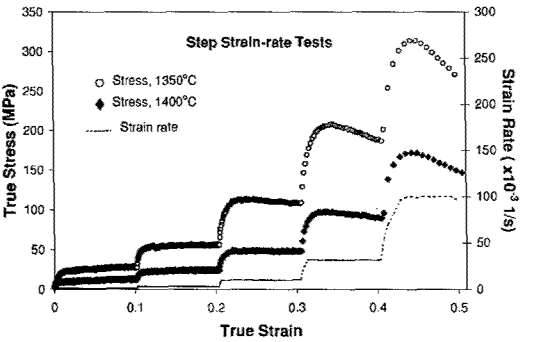

Figure 4. Typical stress-strain curves in the step strain-rate tests

With increasing strain-rate, the trend of shifting from strain hardening to softening can be observed. It is also noticed that this occurs at a higher strain rate if the deformation temperature is higher. The stress-strain rate dependence as measured with step strain rate tests as in Fig. 4 were plotted into double logarithmic charts as in Fig. 5. The slope of the data gives the values of strain rate sensitivity, m. The superplastic deformation of the present material gives a very consistent m value of about 0.55. The constitutive relation for superplastic deformation can be expressed in the form of Mukherjee-Bird-Dorn equation

$$\dot{\varepsilon} = A\frac{D_0 Gb}{kT}\left(\frac{b}{d}\right)^p\left(\frac{\sigma}{G}\right)^n \exp(-Q/RT) \qquad (1)$$

in which G is the elastic modulus, b is the Burgers' vector, k is Boltzmann's constant, T is the absolute temperature, d is the grain size, p is the grain-size dependence coefficient, n is the stress exponent, Q is the activation energy for diffusion, D_0 is a constant and R is the gas constant. The inverse of strain rate sensitivity, m, gives the value of n. The experimentally determined stress dependence of the strain rate n is equal to 2 for this material. This observation narrows the deformation mechanism to two possible choices: (1) Grain boundary sliding accommodated by diffusion, where the interface reaction at grain boundaries controls the deformation rate, as described by Artz-Ashby-Verrall model; (2) Grain boundary sliding accommodated by climbing of lead dislocation in pile-ups in individual grains (Mukherjee model) or in a group of grains (Ball-Hutchison model). The discrimination between these two types of deformation mechanisms requires the determination of other characteristic parameters, namely activation energy Q and grain size dependence p. It is also noticeable in Fig. 5, that for lower temperatures the stress-strain rate curves deviate from the $m = 0.55$ ($n \approx 2$) regime at the high strain-rate end and takes a lower value of strain rate sensitivity. In metals this phenomenon is frequently encountered and is attributable to the transition of mechanism from grain boundary sliding controlled superplasticity to dislocation-climb controlled power-law creep, which has a typical n value of 3-5. In ceramics, the observation of this phenomenon is very rare. In contrast the n value in ceramics, e.g., alumina and zirconia, was found to shift from 2 to 1 as stress and strain rate approach higher values [16,17]. It will be important to find out the reason for this behavior in the present material and this is the subject of continuing research in our laboratory.

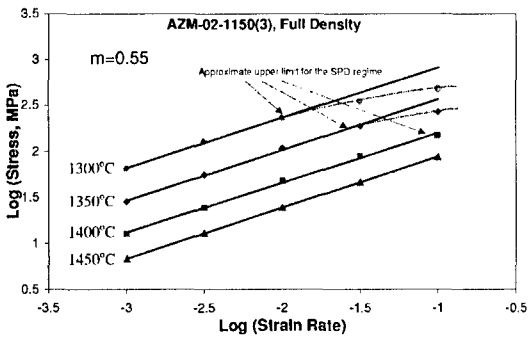

Figure 5. Stress-strain rate relationship, determination of strain rate sensitivity

The dependence of strain rate on temperature at different stress levels (these stress levels were chosen to make sure the deformation is in the m=0.55 superplastic regime) is given in Fig. 6. The activation energy for the superplastic deformation of the $Al_2O_3/ZrO_2/MgAl_2O_4$ composite gives a consistent value of 620 kJ/mol. However, the effort to interpret this activation energy encounters difficulty, mainly owing to the wide scatter of data in the literature concerning the component phases for this material. For instance, for yttria-stabilized zirconia alone, the activation energy for superplastic deformation ranges from 360 to 660 kJ/mol [18]. While in the meantime the activation energy for lattice diffusion of the slower moving cations are 391kJ/mol for Zr^{4+} and 423kJ/mol for Y^{3+}. The grain boundary diffusion activation energy takes values of 309kJ/mol and 293kJ/mol for Zr^{4+} and Y^{3+}, respectively [19]. These values provide poor correlation between phenomenology of superplastic tests and basic diffusion processes. Similar controversies exist for the other two components, alumina, and spinel. More effort on sieving out the literature data, in terms of the differences in purity content, processing route, testing technique as well as microstructural evolution, needs to be conducted. In order to understand the deformation mechanisms in truly nanocrystalline nanocomposites, ongoing investigation to establish the parameter p, the grain size dependence of strain rate, and identify the possible dislocation activities in the deformed samples, is currently underway.

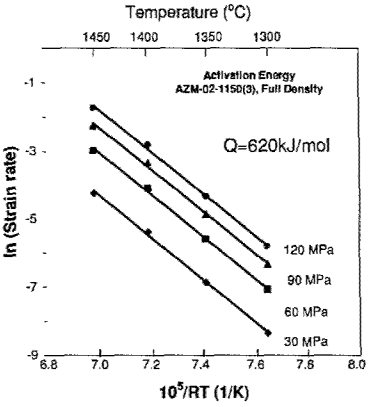

Figure 6. Temperature dependence of strain rate and constant stress.

CONCLUSIONS

(1) This study for the first time demonstrates that ropes of single-wall carbon nanotubes are attractive materials for reinforcement of nanoceramics. The spark-plasma-sintering technique has been found to be a very effective processing method for consolidation of carbon nanotubes composites without accumulating damage. A fracture toughness of 9.7 $MPam^{1/2}$, nearly three times that of pure nanocrystalline alumina, has been achieved in the 10 vol.% $SWCN/Al_2O_3$ nanocomposite. The effective bonding of the SWCN ropes with the matrix plays a central role in the reinforcing effect.

(2) The nanocrystalline $Al_2O_3/ZrO_2/MgAl_2O_4$ ceramic nanocomposite exhibits high-strain-rate superplasticity up to 10^{-1} s^{-1} as low as 1400°C with strain rate sensitivity of 0.55 and activation energy of 620 kJ/mol. These results suggest that grain boundary sliding is the likely mechanism for superplasticity in this nanocomposite.

ACKNOWLEDGEMENTS

This investigation was supported in part by a grant (#G-DAAD 19-00-1-0185) from U.S. Army Research Office with Dr. William Mullins as the Program Manager and in part by the Office of Naval Research grant number N00014-01-C-0370 under contract to Rutgers University. TEM images were obtained at the National Center for Electron Microscopy (NCEM) at the Lawrence Berkeley Laboratory.

REFERENCES

1. G.-D. Zhan, J. D. Kuntz, J Wan, and A. K. Mukherjee, *Nature Materials*, **2**, 38, 2003.
2. P. Calvert, *Nature*, **357**, 365 (1992).
3. S. Subramooney, *Adv. Mater.* **15**, 1157 (1998).
4. M-F. Yu, B. S. Files, S. Arepalli, and R. S. Ruoff, *Phys. Rev. Lett.* **84**, 5552 (2000).
5. O.D. Sherby, T. G. Nieh and J. Wadsworth, *Mater. Sci. Forum*, **243-245**, 11 (1997).
6. T. G. Langdon, *Mater. Sci. Forum*, **304-306,** 13 (1999).
7. B. N. Kim, K. Hiraga, K. Morita and Y. Sakka, *Nature*, **413,** 288 (2001).
8. K. Morita, K. Hiraga, and Y. Sakka, *J. Am.Ceram. Soc.*, **85,** 1900 (2002).
9. M. J. Bronikowski, P. A. Willis, D. T. Colbert, K. A. Smith, and R. E. Smalley, *J. Vac. Sci. Technol.* **19**, 1800 (2001).
10. P. Nikolaev, et al. *Chem. Phys. Lett.* **313**, 91 (1999).
11. G. R. Antis, P. Chantikul, B. R. Lawn, and D. B. Marshall, *J. Am. Ceram. Soc.*, **64**, 533 (1981).
12. Ch. Laurent, A. Peigney, O. Dumortier, and A. Rousset, *J. Euro. Ceram. Soc.* **18**, 2005 (1998).
13. R. Z. Ma, J. Wu, B. Q. Wei, J. Liang, and D. H. Wu, *J. Mater. Sci.* **33**, 5243 (1998).
14. R. W. Siegel, et al. *Scripta Mater.* **44**, 2061 (2001).
15. E. Flahaut, et al. *Acta Mater.* **48**, 3803 (2000).
16. R. M. Cannon, W. H. Rhodes and A. H. Heuer, *J. Am. Ceram. Soc.*, **63,** 46 (1980).
17. L. Clarisse, R. Baddi, A. Baille, J. Crampon, R. Duclos and J. Vicens, *Acta mater.*, **45,** 3843 (1997).
18. M. Gust, G. Goo, J. Wolfenstine and M. L. Mecartney, *J. Am. Ceram. Soc.*, **76,** 1681 (1993).
19. Y. Oishi, K. Ando, and Y. Sakka, in *Advanced Ceramics, **Vol.7**, Additives and Interfaces in Electronic Ceramics*. Edited by M. F. Yan and A. H. Heuer. American Ceramic Society, Columbus, OH, pg. 208 (1993).

Correspondence and requests for materials should be addressed to A. K. Mukherjee. akmukherjee@ucdavis.edu